Effect of biodiesel blends on the regeneration behaviour of Diesel Particulate Filters

D.N. Tziourtzioumis and A.M. Stamatelos

Laboratory of Thermodynamics & Thermal Engines, University of Thessaly, 38334 Volos, Greece, stam@uth.gr

Abstract

An experimental study of the effect of a low percentage biodiesel blend on the diesel filter loading and fuel additive – assisted regeneration behaviour on a conventional, single cylinder engine is presented. The evolution of regeneration is studied by means of infrared thermography on a small filter module. Two sets of regeneration experiments, one for each fuel blend used, with high level of exhaust gas flow rate (normalized per filter volume) and markedly different levels of soot loading were performed. The test fuels were conventional diesel (denoted as B0) and B20 biodiesel blend. The main objective was to investigate the catalytic soot ignition and regeneration propagation when the engine is fuelled by biodiesel blends. Special focus was on the temperature distribution across the filter channels and the evolution of the regeneration at the central and peripheral part of the filter. The results indicated a faster evolution of the regeneration with lower overall filter wall temperatures with favourable effects on the filter durability, when the engine is fuelled by B20.

Introduction

The effect of biodiesel blends on the performance and emissions of Diesel engines is the subject of numerous published research works since 1980. The combustion of biodiesel in engines equipped with conventional fuel injection systems normally results in advancement of the start of injection and combustion, due to differences in chemical and physical properties of the fuels. Unit injector or common rail injection engines do not exhibit the same behaviour. Combustion of biodiesel blends reduces CO, HC and PM emissions, both in older and modern diesel engines, depending also on the specific quality of biodiesel employed.

The Diesel Particulate Filter (DPF) is standard in modern Diesel passenger cars. This technology is associated with increased backpressure from the stored soot and a fuel economy penalty, that should be minimized. Knowledge of soot reactivity in the DPF is important in achieving optimal control and long durability of these devices.

Previous studies point to improved DPF performance by the use of biodiesel blends. The reactivity of diesel particulate is an important factor affecting DPF performance. While few studies examined fuel property effects on soot reactivity, several studies examined soot chemistry and morphology as they relate to the behaviour of biodiesel-derived soot oxidation (Williams et al. 2006; Song et al. 2006; Boehman, Song, and Alam 2005). Engine operating conditions affect the nanostructure of the particles and hence their reactivity. (Zhu et al. 2005) found that the particulate showed amorphous structure at low engine loads and graphitic structures at high loads. Particulate composition is an important factor affecting particle oxidative reactivity. Volatile matter such as hydrocarbons that fill the micro pores on the particulate is a source of further micro pore development and improved reactivity (Stanmore, Brilhac, and Gilot 2001). Fuel-borne catalysts, such as cerium, iron and platinum based compounds, have been employed to increase the reactivity of particulate matter. The alkali metals that can result from the production of biodiesel are also known to catalyze carbon oxidation.

Inserted thermocouples are usually employed to measure local temperature rise during the PM combustion (Schmidt et al. 2007; Haralampous, Koltsakis, and Samaras 2003). These local measurements do not provide adequate information on the dynamic features of the combustion and the spatial temperature distribution in the channel, not being able to distinguish between a moving high temperature front emanating from a single ignition point or that emanating from one of several ignition points. The main advantage of infrared (IR) temperature measurements is that they provide direct information on the combustion mode on the dynamic features of the high temperature zones generated at various ignition sites. A disadvantage of the IR measurements is that the IR camera may only see an external surface of the filter that must be uninsulated. Nevertheless, they provide useful information on dynamic features of the regeneration process. Detailed infrared analysis on a planar DPF under sudden changes in soot feed conditions are

presented by (Martirosyan, Chen, and Luss 2010). Comparative experiments with infrared analysis on a full scale DPF using B0 and B20 biodiesel blends are presented here, aiming at improved understanding of the effect of biodiesel blends on the regeneration behaviour.

Experimental setup

The tests were performed on a SiC DPF fitted to the exhaust of a single cylinder, Diesel engine (Table 1) (Tziourtzioumis 2012), 600 mm downstream the exhaust manifold. The engine is coupled to a 6 kVA electric generator loaded with a set of four 1.5 kW- resistors. Temperatures were measured at the exhaust pipe 80 mm downstream exhaust manifold, at filter inlet and at 2 positions inserted at 25 mm from the filter exit. A/F ratio was measured by an UEGO sensor. Filter loading was measured with a differential pressure transducer. DPX-9 fuel additive was used with a dosimetry of 50 ppm Ce in fuel, due to the relatively low exhaust temperatures at filter inlet, and the lack of active regeneration (e.g. post-injection etc). Figure 1 presents the experimental layout along with the infrared thermography setup. Infrared video acquisition and frame –by- frame analysis were conducted by means of ThermaCAM Researcher Pro software (FLIR 2007). (Table 2). Infrared video acquisition process was triggered during regeneration (3-6 min duration).

Table 1. RF91 Engine technical data and diesel filter specifications.

Engine type	1-cylinder, DI, 4- stroke, naturally aspirated Diesel
Bore x Stroke	90 x 75 mm
Rated power	7 kW @ 3600 rpm
Rated torque	25 Nm @ 2500 rpm
Compression ratio	18.5:1
Filter type	SiC (19/200 cpsi)
Filter side width x side length x length	34 mm x 34 mm x 150 mm
Cell pitch/ Filter wall thickness	1.89 mm/ 0.4 mm

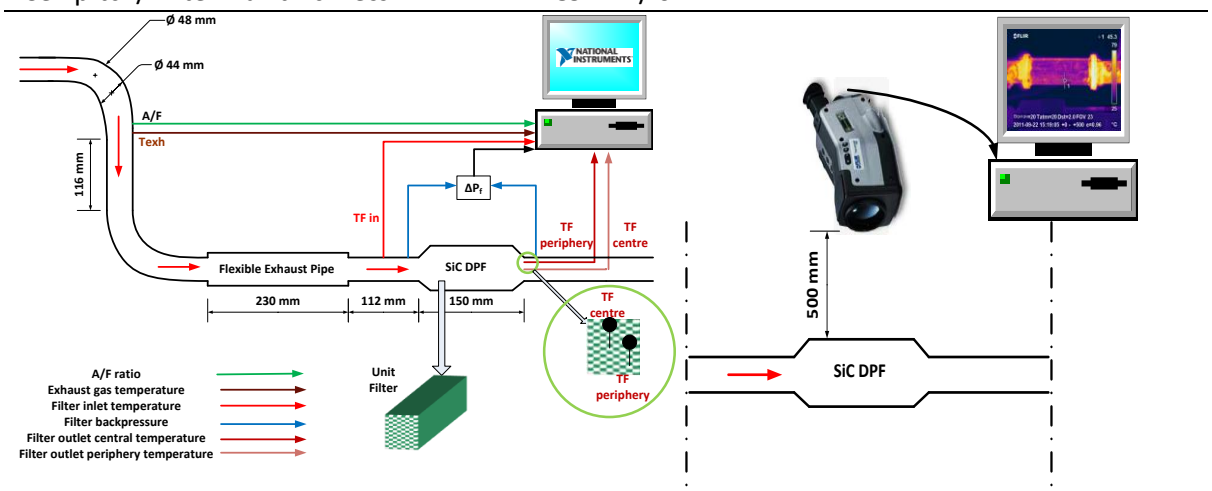

Figure 1. Experimental layout of the exhaust line instrumentation with the main diesel filter measurement points, data acquisition (left) and infrared regeneration video acquisition (right).

Table 2. ThermaCAM S45 main specifications.

Field of view/min focus distance	24°x18^{o}/0.3 m (with 35 mm lens)
Image frequency	50/60 Hz non-interlaced
Detector type	Focal Plane Array (FPA), uncooled microbolometer 320x240 pix
Spectral range	7.5 to 13 μm
Temperature range	-40 ^{o}C to + 1500 ^{o}C
Accuracy	+/-2 ^{o}C, +/-2% of reading

The test fuels are pure Diesel (EN 590), and a blend of 20 vol.% biodiesel (a fatty acid methyl ester produced by 40% rapeseed oil, 30% soybean oil and 30% recycled cooking oils) with pure Diesel. Fuels' specifications are presented in Table 3.

Table 3. Comparison of the main fuel properties, between biodiesel and diesel fuel.

Specifications / ranges	Biodiesel (FAME)	Diesel fuel
Density (15 °C) [kg/m^3]	865	825
Viscosity (40 °C) [cSt]	4.7	2.5
Cetane number	55	50
Cold filter plugging point [°C]	-3	-12
Gross heating value [MJ/kg] (measured)	40.3	46.1
Lower heating value[(MJ/kg] (calculated)	37.7	43.3
Water content [mg/kg]	330	-
Acid number [mg KOH/g]	0.16	-
Sulfur content [ppm]		50
Iodine number g iodine/100g	117	-

Filter loading test protocol

First a mapping process was performed to assess the engine exhaust gas temperature, central channel filter temperature and A/F ratio in the low, medium and high load engine operating range, to find appropriate operation points for filter loading. The final choice was based on filter wall temperature levels and backpressure increase rate. The assessment cycle contains 7 operation points, ranging from 1900 to 3250 rpm and 10.7 to 22.7 Nm load. The last operation point, 3250 rpm/16.2 Nm, with a filter center wall temperature of 375 °C, A/F=35 and filter backpressure increase rate of 2.8 mbar/min, was the one selected for filter loading, both for the B0 and the B20 fuel. The loading test protocol consists of 450 s engine warm-up at 2000 rpm/ 11.9 Nm, followed by 200 s at 2600 rpm/ 12.7 Nm. Finally, the engine accelerates to 3250 rpm/ 16.2 Nm and stays there until filter wall temperatures reaches 370 °C. During loading, the central filter wall temperature is increased from 120 °C to 370 °C and the maximum reported filter backpressure was 235 mbar. Comparison of the two monitored filter wall temperatures shows that the periphery was about 5 °C cooler. The same difference was reported with B20. Because of this temperature gradient, one would expect the VOF content to be somewhat higher at the periphery (Tziourtzioumis and Stamatelos 2012). Filter wall temperature is the critical parameter for the initiation of soot oxidation since it is the main factor affecting the adsorption-desorption phenomena that determine the filter soot VOF content. Whenever the filter wall temperature exceeds 380-420 °C, most VOF is vaporized and only dry soot remains on the filter wall. On the other hand, prolonged operation of a heavily loaded filter with dry soot under low load and speed conditions can lead to re-adsorption of heavy hydrocarbons emitted in the particulate layer, thus increasing its VOF content. Based on previous results (Stratakis 2004), one could assume that under these conditions the filter is loaded with soot at a low-to-medium VOF content, gradually enhancing its oxidation reactivity.

Results and discussion

Two regeneration experiments, one for each fuel, are selected for comparative presentation. The experiments and their main characteristics, like fuel mass consumed during loading and temperatures at filter inlet and inside filter exit (central and peripheral channel) are summarized in Table 4. Filter wall temperatures during loading lie below the VOF oxidation temperature range of 380 to 420 °C.

Table 4.Test protocol of the loading and catalytic regeneration experiments.

#	Fuel Consumed [kg]	TF in [°C]	TF centre [°C]	TF periphery [°C]
B0-01	1.43	367	345	341
B0-02	1.38	369	360	355
B20-01	1.57	360	330	326
B20-02	1.42	355	332	329
B20-03	1.26	370	351	347
B20-04	1.08	372	359	355
B20-05	0.99	358	331	326
B20-06	0.76	355	331	325
B20-07	0.67	416	406	+398

Comparative results are presented in the form of a graph and a sequence of 18 infrared images, covering the duration of regeneration. First, diesel soot oxidation is studied with the filter loaded by the consumption of 1.43 kg fuel, at 3250 rpm/ 16.2 Nm (B0-50 ppm Ce) (Figure 2). The convective heating is dominant in the initiation and propagation of soot oxidation. Due to the high flowrate, the filter is heated quickly and a fast regeneration is achieved. Significant soot oxidation is observed at 380 ^{o}C, resulting to a filter backpressure drop of 92 mbar in 102 s, or 0.9 mbar/s. Temperatures at the periphery are about 13 ^{o}C lower, due to DPF heat losses. Maximum filter central and peripheral wall temperatures of 540 and 527 ^{o}C respectively are measured 110 s after the onset of regeneration. No significant delay between the central and peripheral channels is observed. The respective sequence of infrared images is presented in Figure 3. Frames (e) and (k) show filter wall temperature transition from the selected thresholds of 330 and 370 ^{o}C, respectively.

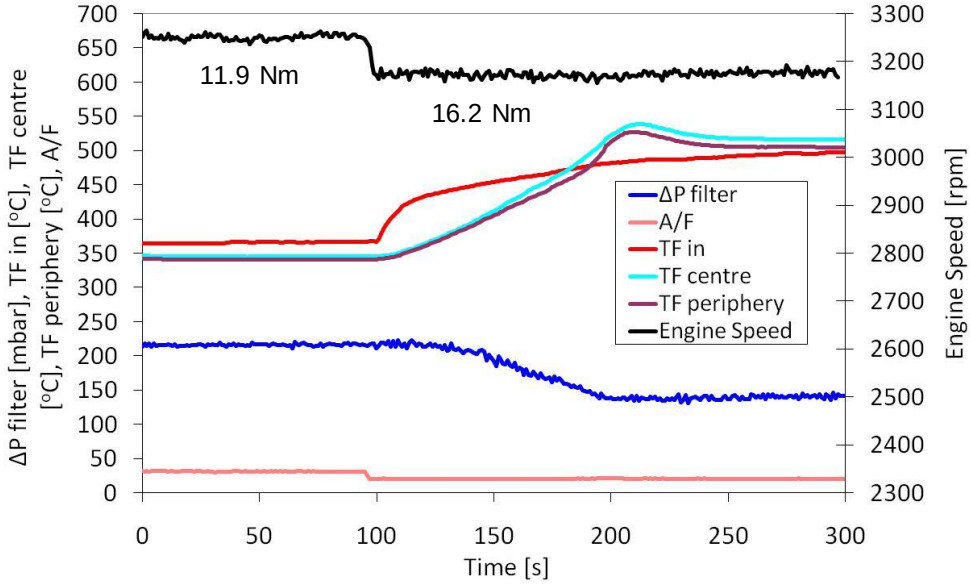

Figure 2 B0-01. Regeneration of a loaded filter (1.43 kg consumed fuel with 50 ppm Ce). Filter temperatures near the exit of a central and a peripheral channel, A/F ratio, engine speed and torque, filter inlet temperature and filter backpressure are presented.

The transition from $T_{surf,max}$ = 330 to 370 ^{o}C is completed in 43 s. The monitored filter surface is separated in 4 sections, for better visualization of the regeneration. According to Figure 3, the regeneration propagates by means of 2 wave fronts, presented by 7 frames each, from (e) to (k) and from (l) to (r) respectively. During the propagation of the first wave front, the regeneration starts in the middle section of the filter, creating 2 hot spots of 340 ^{o}C, as shown in frame (h), which are moving and growing downstream, frame (l), and finally cover the largest part of the monitored filter's surface as presented in frame (k). The second wave front starts from the 3rd section of the filter, further downstream than the 1st wave front, and moves upstream, in line with what is reported by other researchers. Regeneration experiments were carried out at different loading and filter inlet temperature levels, with results summarized in Table 5.

Table 5. Results from the processing of infrared images in the case of B0-50 ppm Ce- doped fuel.

Fuel	Fuel consumed [kg]	Regeneration duration [s]	Regeneration rate [mbar/s]	Transition time from $T_{surf,max}$ = 330 to 370 ^{o}C
B0-02	1.38	120	0.6	57
B0-01	1.43	102	0.9	43

Based on these results, the increase of filter loading between B0-02 and B0-01, induced a decrease of the regeneration duration and transition time between the thresholds of 330 ^{o}C and 370 ^{o}C. Moreover, it induced a significant increase in the filter backpressure reduction rate.

Shifting to the study of B20 fuel behaviour, a characteristic regeneration experiment with the B20-50 ppm Cerium doped fuel is selected as a presentation example. The experimental results are summarized in Table 4. Filter wall temperatures during loading lie below the VOF oxidation temperature range of 380–420 ^{o}C. A regeneration at 3250 rpm/16.2 Nm with the engine operating on B20-50 ppm Ce is presented in Figure 4. A simultaneous elevation of the temperatures at the center and periphery near filter exit peaking at 205 s is observed..

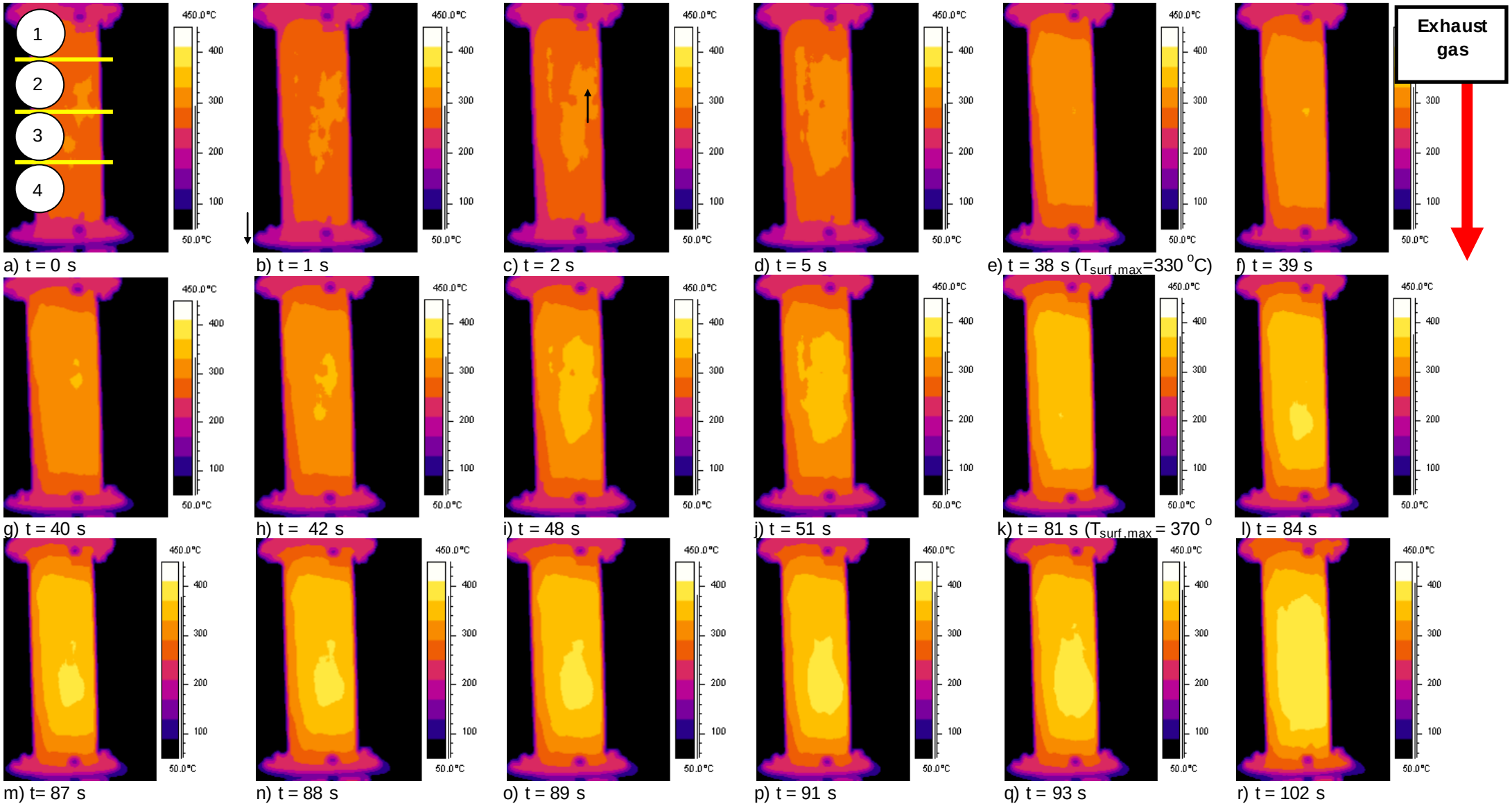

Figure 3 B0-01. Sequence of infrared thermograms of a regeneration with B0-50 ppm fuel. Total regeneration duration of 102 s, transition from 330 to 370 °C in 43 s.

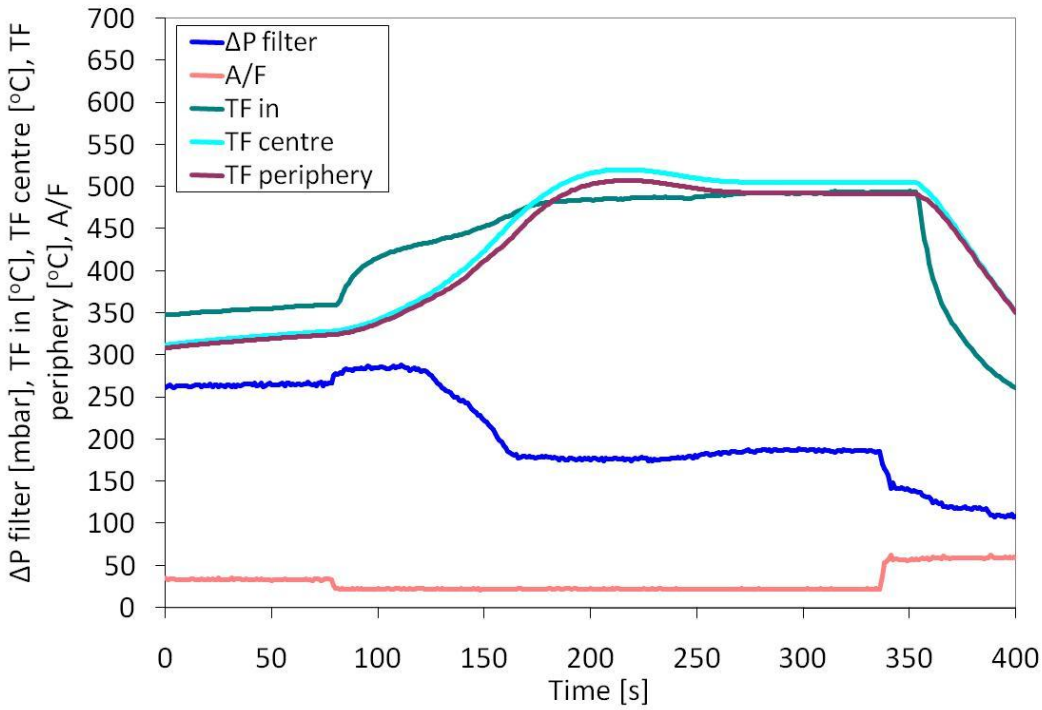

Figure 4 B20-01. Regeneration of a filter loaded (1.57 kg consumed fuel mass) with B20 biodiesel blend soot emitted by the engine operating with 50 ppm Ce doped fuel. Filter exit temperatures of a central and peripheral channel, A/F ratio, filter inlet temperature and backpressure are presented.

Soot oxidation becomes clearly observable when temperature levels exceed 335 ^{o}C, resulting to a backpressure drop of 114 mbar in 94 s, or 1.2 mbar/s. Temperatures at the periphery are about 13 ^{o}C lower. Maximum filter central and peripheral wall temperatures of 520 and 507 ^{o}C respectively are reported 136 s after the onset of regeneration, at 216 s. No significant delay between the onset of regeneration at the central and peripheral channels is observed. Frames (a) and (k) show the temperature transition of filter's wall from the selected thresholds of 330 - 370 ^{o}C, which was completed in 30 s. According to Figure 5, the regeneration is observed to propagate by means of 2 fronts, presented by 7 frames each, from (e) to (k) and from (l) to (r) respectively. Another observation is related to the appearance of hot spots at various positions on the filter's monitored surface. There are 2 regeneration zones. The 1st front starts from the 2nd section of the filter, frame (d), creating a hot core of 330 ^{o}C and propagating downstream with the exhaust gas flow. The same behaviour is reported for the 2nd front but with a different core temperature, 370 ^{o}C. Hot spots are clearly observable in frames (c), (m) and (p). Frame by frame regeneration analysis results with experiments at different soot loading levels are summarized in Table 6.

Based on these results, the increase of filter loading between B20-06 and B20-01 induced a decrease of regeneration duration and transition time between 330 and 370 ^{o}C, along with an increase in backpressure reduction rate. Soot oxidation initiates at about 380 ^{o}C - 420 ^{o}C (using B0-50 ppm Ce) and 330 ^{o}C - 420 ^{o}C, (using B20-50 ppm Ce). Temperatures at the periphery were about 13 ^{o}C lower. There were 2 regeneration fronts, starting from the 2nd and 3rd section of the filter, respectively. A possible explanation could be related to the high levels of superficial velocity (small filter size). The heat generated by the reaction further heats the exhaust gas, causing ignition somewhere downstream. The reaction front moves subsequently in an upstream direction.

Table 6. Results from the processing of infrared images with B20-50 ppm Cerium doped fuel.

Fuel	Fuel consumed [kg]	Regeneration duration [s]	Regeneration rate [mbar/s]	Transition time 330 to 370 ^{o}C	Transition time 370 to 410 ^{o}C
B20-07	0.67	189	0.53	101	70
B20-06	0.76	181	0.51	130	-
B20-05	0.99	177	0.68	45	-
B20-04	1.08	129	0.56	57	-
B20-03	1.26	65	1.34	-	-
B20-02	1.42	120	0.96	55	-
B20-01	1.57	94	1.2	30	-

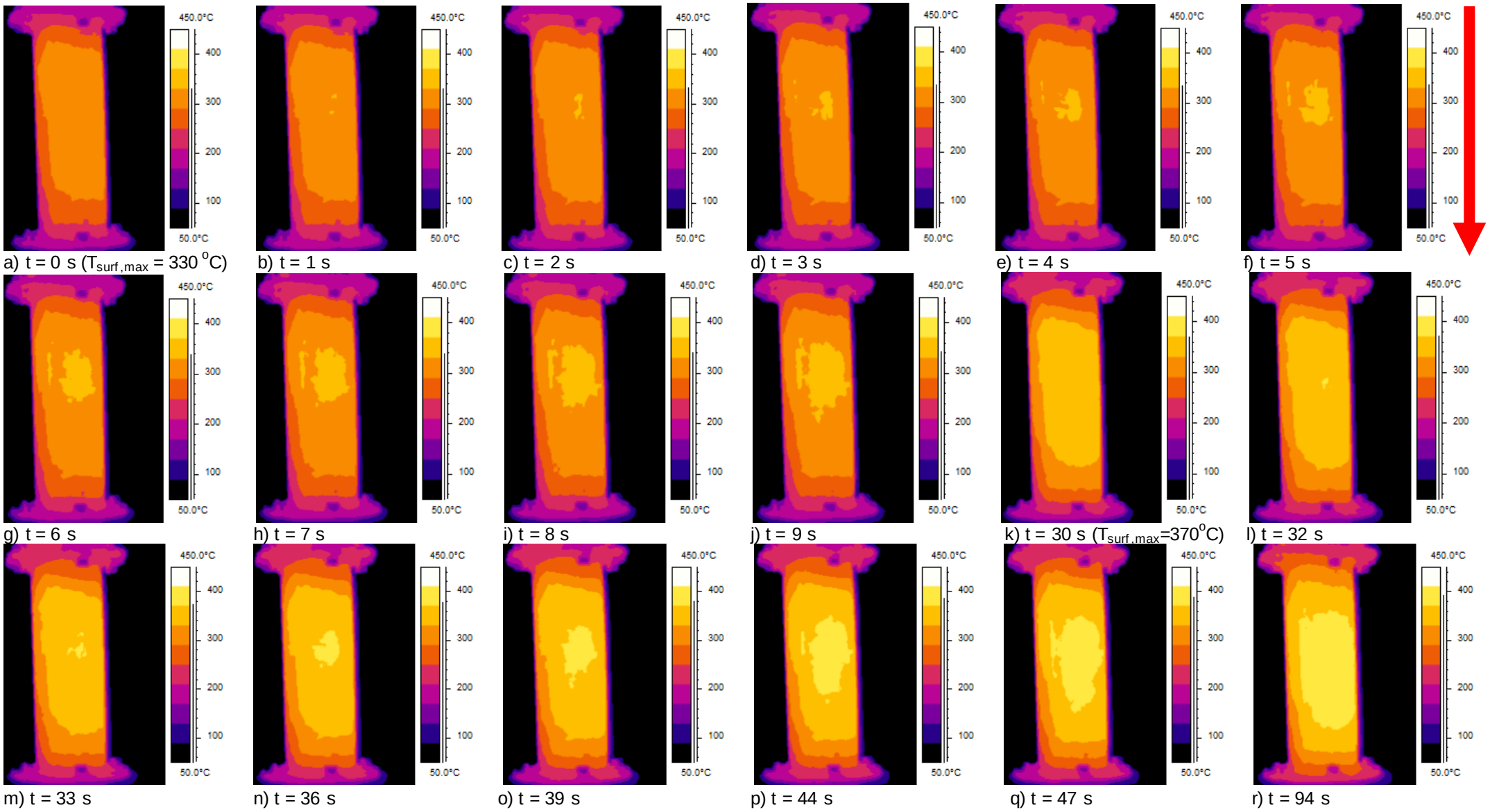

Figure 5 B20-01. Sequence of thermograms of a regeneration with B20-50 ppm fuel, with total duration of 94 s and temperature transition from Tsurf,max = 330 to 370 °C in 30 s.

Conclusions

A comparison of the DPF regeneration behaviour of a conventional single cylinder engine with B0 and B20 as a fuel indicates equivalent levels of maximum filter temperatures. However, comparison of the evolution of the respective sets of thermograms taken along one lateral face of the filter indicates that filter temperatures at the periphery are significantly higher with B20. Detailed video analysis shows faster and more complete regenerations with the B20, in line with is reported from other researchers. The faster evolution of regeneration with lower overall filter wall temperatures is also favourable on filter durability and fuel economy grounds. This fact, combined with the reduced black carbon particulate emissions, suggest that an increase from the 5-7% biodiesel blend ratios of today up to 20% would be worthwhile for the DPF.

Acknowledgments

Financial support by “Alexander S. Onassis” Public Benefit Foundation (doctoral scholarship, D. Tziourtzioumis, 2009-2011) and the Hellenic General Secretariat of Research and Technology (“RIP A6-Production of biofuels in Thessaly”), is gratefully acknowledged.

References

Boehman, A. L., J. Song, and M. Alam. 2005. Impact of biodiesel blending on diesel soot and the regeneration of particulate filters. *Energy and Fuels* 19 (5):1857-1864.

FLIR. 2007. ThermaCam Reseacher Professional 2.8 SR3.

Haralampous, O. A., G.C. Koltsakis, and Z.C. Samaras. 2003. Partial regenerations in diesel particulate filters. *SAE Technical paper No. 2003-01-1881*.

Martirosyan, K. S., K. Chen, and D. Luss. 2010. Behavior features of soot combustion in diesel particulate filter. *Chemical Engineering Science* 65:42-46.

Schmidt, N, T Root, E Wirojsakunchai, E. Schroeder, C. Kolodziej, D.E. Foster, T. Suga, and T. Kawai. 2007. Detailed diesel exhaust particulate characterization and DPF regeneration behavior measurements for two different regeneration systems. *SAE Technical paper No. 2007-01-1063*.

Song, J., M. Alam, A. L. Boehman, and U. Kim. 2006. Examination of the oxidation behavior of biodiesel soot. *Combustion and Flame* 146 (4):589-604.

Stanmore, B. R., J. F. Brilhac, and P. Gilot. 2001. The oxidation of soot: a Review of experiments, mechanisms and models. *Carbon* 39:2247-2268.

Stratakis, G.A. 2004. Experimental Investigation of Catalytic Soot Oxidation and Pressure-Drop Characteristics in Wall-Flow Diesel Particulate Filters, PhD Thesis, Mechanical Engineering Department, University of Thessaly, Volos.

Tziourtzioumis, D. 2012. Experimental Investigation of the steady state and transient operation of Diesel Engines fuelled by high percentage biodiesel blends. PhD Thesis, Mechanical Engineering Department, University of Thessaly, Volos.

Tziourtzioumis, D. , and A. Stamatelos. 2012. Investigation of the effect of biodiesel blends on the performance of a fuel additive-assisted diesel filter system. *International Journal of Engine Research (under review)*.

Williams, A., R.L. McCormick, R.R. Hayes, J. Ireland, and H. Fang. 2006. Effect of biodiesel blends on diesel particulate filter performance. *SAE Technical Paper No. 2006-01-3280*.

Zhu, J., K. O. Lee, A. Yozgatligil, and M.Y. Choi. 2005. Effects of engine operating conditions on morphology, microstructure and fractal geometry of light-duty diesel engine particulates. *Proceedings of the Combustion Institute* 30:2781-2789.